Dalton Transactions

Article

Synthesis of tris(3-pyridyl)aluminate ligand and its unexpected stability against hydrolysis: revealing cooperativity effects in heterobimetallic pyridyl aluminates

fReceived 00th January 20xx,
Accepted 00th January 20xx

DOI: 10.1039/x0xx00000x

www.rsc.org/

Álvaro García-Romero,[a] Jose M. Martín-Álvarez,[a] Annie L. Colebatch,[b,c] Alex J. Plajer,[d] Daniel Miguel,[a] Celedonio M. Álvarez,[a]* and Raúl García-Rodríguez [a*]

We report the elusive metallic anion $[EtAl(3\text{-py})_3]^-$ (3-py = 3-pyridyl) (1), the first member of the anionic tris(3-pyridyl) family. Unexpectedly, the lithium complex 1Li shows substantial protic stability against water and alcohols, unlike related tris(2-pyridyl)aluminate analogues. This stability appears to be related to the inability of the $[EtAl(3\text{-py})_3]^-$ anion to chelate Li^+, which precludes a decomposition pathway involving Li/Al cooperativity.

Introduction

Neutral and non-metallic tris(2-pyridyl) ligands [E(py)$_3$] (py = 2-pyridyl, Y = CR, COR, CH, N, P, P=O, *etc.*, Fig. 1A) are a large family of ligands that have experienced a resurgence in interest, and their coordination chemistry has been investigated extensively.[1] This interest has been motivated by the important applications this class of ligands have found in fields such as catalysis, organometallic chemistry, modern coordination chemistry and even bioinorganic chemistry.[2–12] Recently, the use of more metallic elements in the tris(2-pyridyl) framework bridgehead to introduce new reactivity and properties has become a focus of interest in this area.[4,13–22] This strategy parallels the use of different main group element bridgeheads, which has emerged as a strategy to modulate the reactivity and structure for a large variety of ligands. [21,23–26]

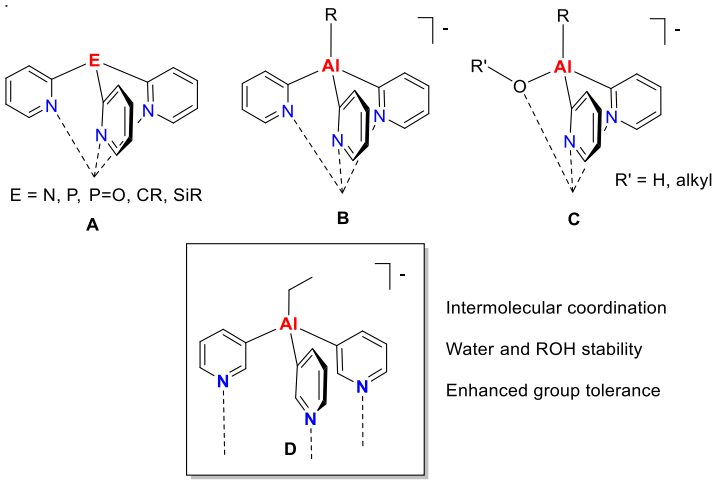

Fig. 1 (a) Conventional, neutral tris(2-pyridyl) ligands containing non-metallic E = N, P, CR, and SiR bridgeheads, **(b)** tris(2-pyridyl)aluminates, **(c)** selective monosubstitution of a 2-pyridyl group by an –OH or –OR group and (d) the elusive tris(3-pyridyl)aluminate ligand reported in this work.

Metallic tris(2-pyridyl)aluminates[27] represent one of the few anionic members of the tris(2-pyridyl) family (Fig. 1B).[28–30] Their negative charge results in high affinities for a wide range of main group[31,32] and transition metals,[33–35] as well as lanthanides.[36,37] They have also found application as catalysts; for instance, [{MeAl(2-py)$_3$}$_2$Fe] shows high catalytic activity in the selective epoxidation of styrene.[33]

The incorporation of a more electropositive (more metallic) bridgehead atom enhances the polarity of the bridgehead–pyridyl bond (Al–C$_{py}$), which in turn causes these aluminate ligands to behave as strong bases. For example, **B** reacts immediately and quantitatively with H_2O and alcohols, undergoing selective replacement of the 2-pyridyl groups by OH or alkoxide groups (Fig. 1C).[38] This selective hydrolysis enables facile post-functionalization of the pyridyl framework, which has led to the development of chiral sensing applications using tris(2-pyridyl)aluminate ligands. For instance, [Li{EtAl(6-

[a] GIR MIOMeT-IU Cinquima-Química Inorgánica Facultad de Ciencias, Universidad de Valladolid; Campus Miguel Delibes, 47011 Valladolid (Spain). E-mail: celedonio.alvarez@uva.es , raul.garcia.rodriguez@uva.es
[b] Chemistry Department. Cambridge University, Lensfield Road, Cambridge CB2 1EW (U.K.)
[c] Research School of Chemistry. Australian National University, Canberra, ACT, 2601 (Australia)
[d] Chemical Research Laboratory 12 Mansfield Road, Oxford, OX1 3TA (UK)
Electronic Supplementary Information (ESI) available: NMR data DFT Calculations and X-ray single-crystal structure solution and refinement details (CCDC 2095751).

Me-2-py)$_3$}] reacts with chiral alcohols in toluene to form diastereomeric dimers [Li{EtAl(6-Me-2-py)$_2$(OR*)}]$_2$ from which the enantiomeric excess (ee) of the alcohol can be determined using NMR spectroscopy, with the 6-Me groups acting as reporter groups (Fig. 2a).[39] In a similar vein, the rare chiral-at-Al aluminate [Li{EtAl(6-Me-2-py)(OMe)(OtBu)}]$_2$ can be produced by stepwise reaction with two different alcohols (Fig. 2b).[40] The high polarity of the bridgehead Al–C bonds has also been associated with the behaviour of tris(2-pyridyl)aluminate lithium salts as nucleophiles (adding to aldehydes, such as Ph–CHO)[41] as well as pyridyl transfer reagents (transferring the pyridyl groups to metal salts such as $SnCl_2$ and CuCl).[27,42] However, this rich reactivity dramatically limits their applicability as bench reagents, as they are incompatible with a large variety of solvents and substrates (*i.e.*, protic solvents or relatively acidic or electrophilic substrates), requiring the use of rigorously dried solvents.

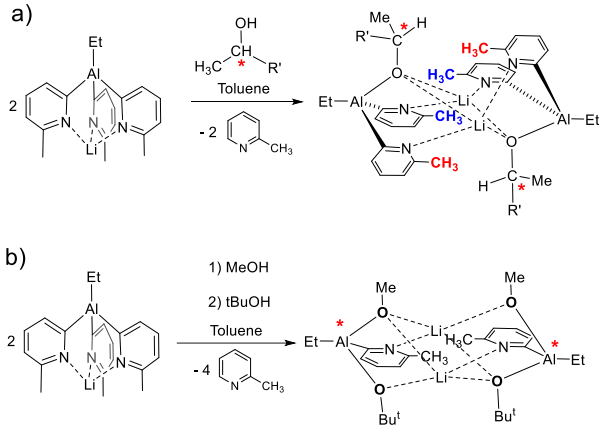

Fig. 2 (a) Reaction of [Li{EtAl(6-Me-2-py)$_3$}] with chiral alcohols and the formation of diastereomeric dimers, with the magnetically inequivalent 6-Me environments highlighted. **(b)** Stepwise reaction of [Li{EtAl(6-Me-2-py)$_3$}] with two different non-chiral alcohols to give a chiral-at-aluminium aluminate.

Tris(pyridyl) ligands based on 3-py groups have clear potential as building blocks and are expected to show radically different behaviour from their 2-py counterparts. The incorporation of the N-donor functionality at the 3-position should result in a change in the character of the ligand from tripodal and intramolecular for tris(2-pyridyl) ligands to intermolecular for tris(3-pyridyl) ligands (cf. Fig. 1A and 1D). However, in contrast to ubiquitous 2-pyridyl-based ligands, ligands containing 3-py functional groups have been largely overlooked. Only a few examples with neutral non-metallic P[43–46] or Si[47] bridgeheads, and, very recently, a metallic (3-pyridyl)stannane, have been structurally characterized.[48] Despite the limited examples of known tris(3-pyridyl) ligands, these (so far) neutral systems have been used in the construction of various supramolecular architectures and have even found applications in catalysis.[46,49–53]

Herein, we report the readily prepared tris(3-pyridyl) aluminate anion [EtAl(3-py)$_3$]$^-$ (**1**), the first anionic member of the tris(3-pyridyl) family. The ability of the ligand to establish supramolecular interactions is seen in the polymeric structure of the "ate complex" Li[EtAl(3-py)$_3$] (**1**Li). Remarkably, unlike its [RAl(2-py)$_3$]$^-$ counterparts, it is stable towards H_2O and other protic compounds such as alcohols and can therefore be used as a bench-stable reagent, despite the presence of highly polar Al–C_{py} bonds.

Results and Discussion

Early attempts to prepare the elusive **1**Li were undertaken in THF following a synthetic route similar to those typically employed for the synthesis of tris(2-pyridyl)aluminates. However, lithiation of 3-Br-py in THF led to black mixtures suggesting decomposition (and a complex mixture of compounds was observed using NMR spectroscopy after reaction with $EtAlCl_2$). The reaction of turbo-Grignard reagent iPrMgCl·LiCl with 3-Br-py and subsequent reaction with $EtAlCl_2$ also led to the formation of an intractable mixture of compounds. Our target compound Li[EtAl(3-py)$_3$] (**1**Li) was finally obtained from the intermediate Li(3-py) using an *in situ* stepwise synthetic route under carefully optimized conditions: Lithiation was carried out in Et_2O at -78 °C followed by reaction of the *in situ* prepared Li(3-py) intermediate with $RAlCl_2$ (3:1) at -78 °C. The lithium salt **1**Li was obtained in moderate yields as large colourless crystals (54%) after workup of the reaction (see Scheme 1 and experimental section). Both the reaction time and solvent utilized in the first lithiation step were found to be critical in the formation of **1**Li, and the crystallization conditions (slow diffusion of toluene in a concentrated solution in THF at 8 °C) were crucial to its successful isolation.

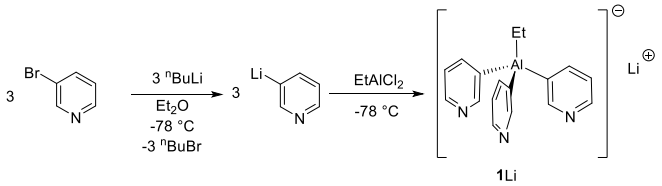

Scheme 1. Synthesis of the complex [EtAl(3-py)]Li (**1**Li).

Compound **1**Li was thoroughly characterized using heteronuclear (^{1}H, ^{13}C, ^{7}Li, and ^{27}Al) NMR spectroscopy. The room-temperature ^{1}H NMR spectrum of **1**Li in DMSO-d_6 shows the presence of an Al-bonded Et group [δ 0.1 ppm (q) and 1.1 ppm (t)] and only one pyridyl environment, suggesting an effective C_{3v} symmetry of the ligand in solution. Full assignment of the resonances was done with the help of 2D experiments. The ^{1}H–^{1}H NOESY experiment was particularly informative, showing the close spatial proximity of the py-H_3 and py-H_6 protons to the Et–Al group, thus confirming the Et–Al–3-py linkage (see ESI). High resolution -ve ion mass spectrometry further confirmed the formation of the anion **1** via the expected [M]$^-$ peak at *m/z* 290.1251 (calcd 290.1243; –2.65 ppm error).

The crystals of **1**Li were not soluble in most organic solvents (THF, toluene, $CDCl_3$ MeCN, acetone), suggesting an extended solid structure, rather than the discrete lithium complexes typically formed by tripodal tris(2-pyridyl) aluminates (Fig. 1B and Fig. 2). This was confirmed by a single-crystal X-ray study. The structure of the lithium salt **1**Li is shown in Fig. 3; **1**Li displays a polymeric structure formed by $[EtAl(3\text{-py})_3]Li{\cdot}THF$ units in which 3-py units from three adjacent molecules coordinate a Li atom. A molecule of THF completes the tetracoordination of the Li. This produces a two-dimensional polymeric structure in which all the 3-py arms are coordinated to Li (Fig. 3b).

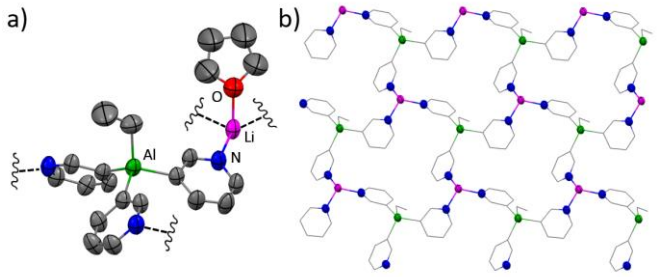

Fig. 3 (a) X-ray crystal structure of the monomer unit of **1** showing displacement ellipsoids at 40%. H atoms are omitted for clarity. Selected bond lengths (Å) and angles (deg): Al–C_{py} 2.010(3)–2.015(2), Al–C_{Et} 1.978(3), N–Li 2.025(4), C_{py}–Al–C_{py} 107.5(1)–108.6(1). Colour key: C (grey), Al (green), N (blue), Li (pink), O (red). **(b).** The 2D polymeric arrangement formed by [EtAl(3-py)]Li units. THF molecules have been omitted for clarity.

The marked insolubility of **1**Li in common organic solvents was expected based on its polymeric structure in the solid state. However, to our surprise, compound **1**Li could be characterized in DMSO-d_6, even in the presence of residual water, without observing any evidence of decomposition, *e.g.*, with no formation of free pyridine resulting from hydrolysis. Indeed, even in the presence of a large excess of H_2O (80 equiv, Fig. 4a), no decomposition was observed after storing the sample for several weeks or heating it to 100 °C for 3 h. More strikingly, **1**Li could be dissolved in wet CD_3OD, and no decomposition was observed after 1 h at room temperature (Fig. 4b). Only prolonged storage in methanol led to its slow decomposition and the appearance of free pyridine (3-D-py) in the ^1H NMR spectrum along with other unidentified species after 2 days (see ESI). In addition to mildly acidic compounds, **1**Li is also stable towards electrophilic compounds such as benzaldehyde (see ESI). This is in sharp contrast to the much higher reactivity of tris(2-pyridyl) aluminates, which can act as strong bases and nucleophiles,[27,38–41] as noted in the introduction.

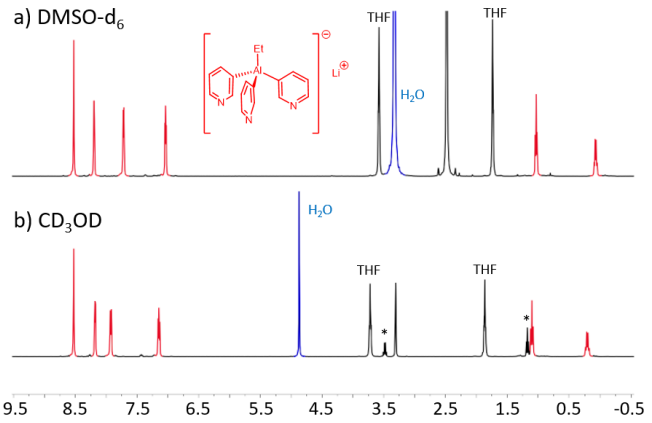

Fig. 4 (a) ^1H NMR spectrum of $[EtAl(3\text{-py})_3]Li$ (**1**Li) in DMSO-d_6 after adding 80 equiv of H_2O. **(b)** ^1H NMR spectrum of $[EtAl(3\text{-py})_3]Li$ (**1**Li) in CD_3OD after 1 h at room temperature. Note: the asterisks represent residual Et_2O signals at 3.49 (q) and 1.18 (t) ppm. No decomposition is observed in any of the experiments.

In apparent contradiction to the experimental observations, model DFT calculations in DMSO as the solvent showed, perhaps not unexpectedly, that the hydrolysis reaction of **1** to give $[EtAl(OH)(3\text{-py})_2]^-$ (the 3-py analogue of EtAl(OH)(2-py) in Fig. 1b) and free pyridine is highly favourable with ΔG = -29.5 kcal/mol (see ESI). Additional DFT calculations were carried out to assess whether the kinetic inertness of the tris(3-pyridyl)aluminate against H_2O and ROH was symptomatic of the lower polarity of the Al–C_{3py} bond as compared to Al–C_{2py}. NBO atomic natural charges were calculated for the optimized geometries of $[EtAl(3\text{-py})_3]^-$ (**1**) and its 2-py analogue $[EtAl(2\text{-py})_3]^-$ (**2**) (Fig. 2b). To our surprise, the Al–C_{3py} bond in **1** is even more polarized than the Al–C_{2py} bond in **2**. Specifically, the difference between the atomic charges at the Al atoms and the bonded C_{py} atoms are 2.07 and 1.72 for **1** and **2**, respectively (Fig. 5). Moreover, Li^+ coordination does not substantially affect the Al–C polarity in **1**, with the calculated differences in atomic charges being 1.72 and 1.59 for Al–C_{2py} in **1** and **1**Li, respectively (See ESI). As expected, little change is observed in the polarity of the Al–C_{Et} bond moving from **1** to **2**, and the calculations reveal that this bond is actually more polarized than the Al–C_{py} bond (charge differences of 2.51 and 2.47, respectively). These results suggested that kinetic factors might explain the inertness of **1**Li in comparison with **2**Li towards hydrolysis.

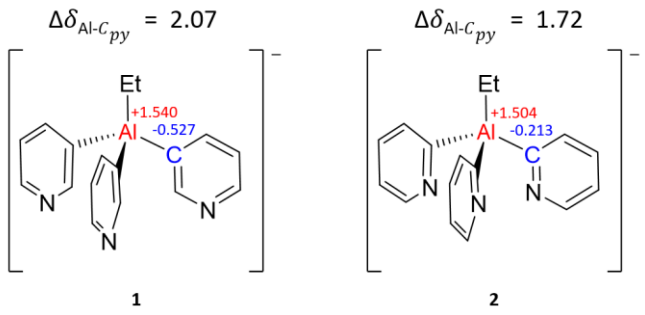

Fig. 5 NBO atomic natural charges and Al–C_{py} bond polarity comparison between $[EtAl(2\text{-}py)_3]^-$ and $[EtAl(3\text{-}py)_3]^-$ anions obtained from DFT calculations. The Al–C_{py} bond in $[EtAl(3\text{-}py)_3]^-$ is more polarized than the Al–C_{py} bond in $[EtAl(2\text{-}py)_3]^-$.

Information regarding structure in solution is crucial to rationalize reactivity, particularly in bimetallic systems, in which close proximity of the two metals might lead to cooperativity. Thus, to study the aggregation state of **1**Li in DMSO solution, we performed DOSY NMR experiments. The ^{1}H signals for the aluminate have a diffusion coefficient (*D*) of 2.42 ± 0.01 × 10^{-10} m^2 s^{-1}, while the ^{7}Li DOSY NMR presented a *D* of 2.23 ± 0.03 × 10^{-10} m^2 s^{-1}. Although similar, the two diffusion coefficients are distinctly different, suggesting that **1**Li does not form a contact ion pair (CIP) in DMSO and pointing towards ion separation (Fig. 6).

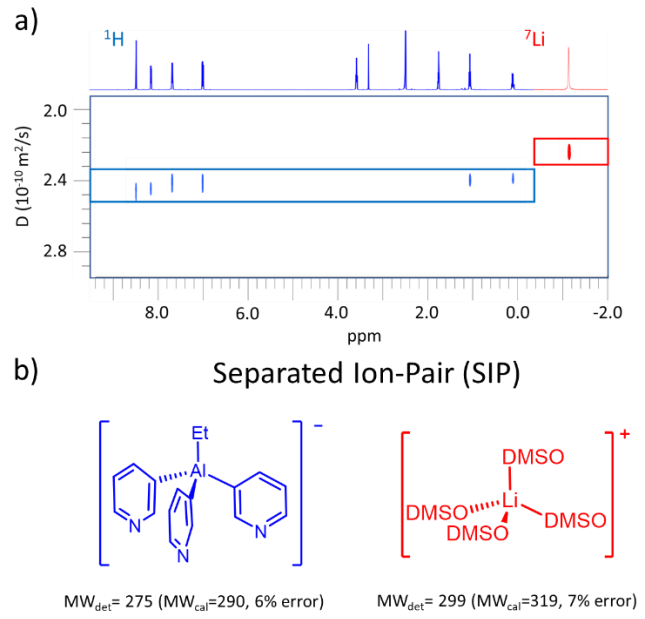

Fig. 6 (a) Superposition of ^{1}H (blue) and ^{7}Li (red) DOSY NMR spectra of $[EtAl(3\text{-}py)_3]Li$ (**1**Li) in DMSO-d_6 at 298 K. Note that the aluminate resonances of **1**Li in the ^{1}H DOSY exhibit a distinctly higher diffusion coefficient (2.42 × 10^{-10} m^2 s^{-1}) than that observed in the ^{7}Li DOSY (2.23 × 10^{-10} m^2 s^{-1}). **(b)** Separated ion pair for **1**Li in DMSO solution, showing their MW_{det} using the DOSY Stalke method and comparison with the expected MW_{cal} for each species.

To obtain further information, the molecular weight was determined (MW_{det}) from the ^{1}H DOSY data via two methods: in the presence of three internal standards[54,55] and using the Stalke method.[56–58] The methods gave similar values of 288 and 275 g mol^{-1}, respectively, which agree well with the theoretically calculated MW (MW_{cal}) for the monomeric aluminate $[EtAl(3\text{-}py)_3]^-$ (MW_{cal} = 290, 1% and 6% error, respectively; see ESI). Similar MW_{det} values were obtained from the ^{1}H DOSY data at different concentrations, clearly indicating the collapse of the polymeric structure observed in the solid state (Fig. 3) and the formation of separate $[EtAl(3\text{-}py)_3]^-$ anions in solution in all cases. In contrast to tris(2-pyridyl) aluminates, $[EtAl(3\text{-}py)_3]^-$ (**1**) cannot chelate Li^+ (see Fig. 1), and an unsolvated contact ion pair (CIP) $Li[EtAl(3\text{-}py)_3]$ (MW_{cal} 297) is not likely to form in the absence of steric hindrance at the py ring and in the coordinating solvent DMSO, nor would it be consistent with the different diffusion coefficients (*D*) extracted from the ^{1}H and ^{7}Li DOSY experiments. In addition to these reasons, solvated DMSO contact ion pairs, $(DMSO)_x$–$Li[EtAl(3\text{-}py)]_3$, do not fit with the extracted MW_{det} (for instance, for *x* = 2, MW_{cal} = 454-with an error of 65%, and even for the much less likely monosolvated species *x* = 1, MW_{cal} = 375, with an error of 37%), and can thus be ruled out (see ESI). The MW_{det} obtained from the ^{7}Li data (MW_{det} = 299) fit well with the known tetracoordinated Li-DMSO solvate $[Li(DMSO)_4]^+$ [59] (MW_{cal} = 319, 7% error; Fig 6b); however, the existence of other Li–DMSO solvates in solution cannot be completely ruled out (ESI).

Cooperativity in bimetallic systems has been shown to dramatically change their reactivity. For instance, the basicity of organozinc and organomagnesium compounds can be enhanced by Li mediation, as seen in the iconic case of "Turbo Reagents".[60,61] We propose that the lower reactivity (basi city) observed in bimetallic **1**Li compared to the closely related tris(2-pyridyl)aluminate lithium salts is related to the lack of Li–Al cooperativity, which is disfavored by the formation of separated ion pairs (SIP) in **1**Li. To further stress this point, we revisited the reactivity of $[EtAl(2\text{-}py)_3]Li{\cdot}THF$ (**2**Li), the direct analogue of **1**Li, under the same conditions. As expected, **2**Li reacted immediately and quantitatively with H_2O in DMSO-d_6, leading to the formation of free pyridine and the complete hydrolysis of **2**Li after the addition of just *ca.* 3 equiv of H_2O (see ESI). In contrast with **1**Li, ^{1}H and ^{7}Li DOSY experiments indicate that **2**Li behaves as a CIP in DMSO-d_6, as revealed by the virtually identical diffusion coefficients observed in the ^{1}H (2.03 ± 0.01 × 10^{-10} m^2 s^{-1}) and ^{7}Li (1.99 ± 0.08 × 10^{-10} m^2 s^{-1}) DOSY NMR experiments (Fig. 7). The extracted MW_{det} matches that expected for the CIP $[EtAl(2\text{-}py)_3]Li{\cdot}DMSO$ (3% error) for which Li^+ retains a coordination number of four as seen in the solid state of **2**Li·THF.[32] Moreover, in the ^{1}H–^{7}Li HOESY experiments, the crosspeak between the ^{7}Li and the H_6-py resonances indicates that the Li atom is spatially close to the pyridine H_6 protons in **2**Li (see ESI). Experiments under similar conditions for **1**Li did not provide any crosspeak, and therefore no evidence for proximity between the Li and the aluminate framework, thus providing further support for **1**Li behaving as a SIP and **2**Li as a CIP in DMSO-d_6.

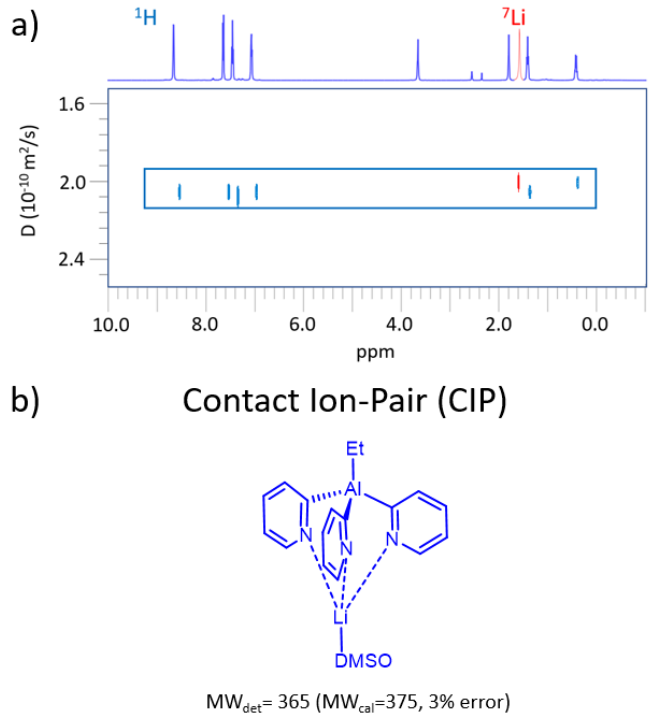

Fig. 7 (a) Superposition of ^{1}H (blue) and ^{7}Li (red) DOSY-NMR spectra of [EtAl(2-py)$_3$]Li in DMSO-d$_6$ at 298 K. Note that the aluminate resonances of **2**Li in the ^{1}H DOSY (2.03×10^{-10} m^2 s^{-1}) show virtually the same diffusion coefficient as that observed in the ^{7}Li DOSY (1.99×10^{-10} m^2 s^{-1}). **(b)** Contact ion-pair for **2**Li in DMSO solution, its MW$_{det}$ using the DOSY Stalke method and its comparison with the expected MW$_{cal}$.

Having established the different natures of **1**Li (SIP) and **2**Li (CIP) in solution, we suggest that the fast hydrolysis in **2**Li (and other tris(2-pyridyl)aluminate lithium salts) is associated with Li–Al cooperativity, which enhances the pyridyl basicity of **2**Li by providing feasible hydrolysis pathways based on the proximity between the two metals, which is more favored in **2**Li due to its chelating nature than in **1**Li. In contrast, the separation of Li and Al in the SIPs of **1**Li precludes such Li–Al-cooperativity-based pathways, resulting in kinetically inert tris(3-pyridyl)aluminates.

To illustrate this idea, model DFT calculations were performed, and showed a plausible mechanism for the hydrolysis of [MeAl(2-py)$_3$]Li. Scheme 2 presents one such possible pathway starting from a CIP. Although the lithium is coordinated to a single DMSO, in the presence of a small amount of water, water can coordinate to Li$^+$. To represent this low-concentration but reactive situation, for calculational simplicity we used [MeAl(2-py)$_3$]Li·(H$_2$O)$_3$ as a model, in which the Li atom coordinates three molecules of water, and two of the pyridines have been displaced, which thus retains the tetracoordination of Li$^+$ (see Scheme 2). Subsequently, a further molecule of water was introduced with the result that it is brought into close proximity to one of the aluminate pyridines by H-bonding with the water coordinated to lithium. This leads to the replacement of the 2-py group with OH and the formation of free pyridine, as observed experimentally. The calculations showed that the hydrolysis reaction is spontaneous (ΔG = –30.7 kcal/mol) and has an accessible activation barrier ($\Delta G^{\#}$ = 19.0 kcal/mol), both agreeing with the fast observed hydrolysis at room temperature for **2**Li (see ESI). Although this model is very simple, it captures a possible pathway based on Li–Al cooperativity, featuring two hydrogen-bonded molecules of water, in which the Lewis acidic Li$^+$ center acts as an anchor point which activates and directs the attack of H$_2$O.

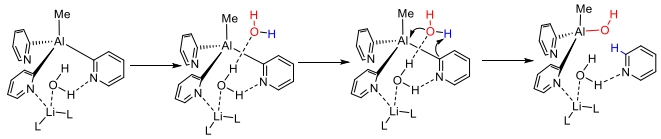

Scheme 2. A plausible reaction pathway for the hydrolysis of [MeAl(2-py)$_3$]Li in DMSO that has been calculated by DFT. Note that the DFT model includes L = H$_2$O for simplicity, although the coordination sphere of Li$^+$ in this reactive species most likely presents DMSO interactions (*i.e.*, L = H$_2$O or DMSO).

Conclusions

The incorporation of the N-donor functionality into the 3 position rather than the 2 position leads to a change in the character of the aluminate ligand from intramolecular and tripodal to intermolecular, as can be seen in the formation of a polymeric 2-D structure for **1**Li in the solid state. This result demonstrates that the newly available 3-py aluminate, which is the first anionic member of the tris-3-pyridyl family, can potentially be used as a ligand for supramolecular chemistry. A less obvious consequence of changing the 2-py groups to 3-py groups is that in contrast to its 2-py aluminate analogue **2**Li, **1**Li is much more kinetically stable in the presence of H$_2$O (or ROH).

DFT studies show that the Al–C$_{3py}$ bond of **1**Li is even more polarized than the Al–C$_{2py}$ bond of its 2-py analogue, and therefore, bond polarity cannot be the only factor responsible for its much lower basicity (and nucleophilicity) compared to **2**Li. The radically different reactivity can be explained by the way in which the intermolecular nature of **1**Li prevents Li–Al cooperativity, in contrast to tripodal **2**Li. We have shown that the aluminate **1**Li in DMSO forms solvent-separated ion pairs that would prevent such cooperativity. Indeed, deprotonation due to pyridyl basicity is completely shut down, and **1**Li is stable in DMSO for a prolonged period, even in the presence of large amounts of H$_2$O. In contrast, **2**Li behaves as a CIP in DMSO, resulting in close proximity of Li and Al, which enables metal cooperation. We propose that the Li$^+$ in 2-py systems can serve as a Lewis acidic centre activating and bringing H$_2$O (or ROH) into close proximity with the aluminate. Therefore, although the high polarity of the Al–C bond has commonly been invoked to explain the strong nucleophilicity and high basicity of tris(2-pyridyl)aluminates, the close proximity of the Li$^+$ and the Al–C$_{py}$ bonds provides a further factor in this understanding.

Our conclusion is an important one since it also suggests that the unique reactivities previously observed in tris(2-

pyridyl)aluminate lithium salts may be dictated, at least in part, by Li-Al cooperativity. We hope this might lead to the rational design of more stable tris(pyridyl)aluminates, as well as the tailoring of their reactivity and selectivity.

Experimental section

General experimental techniques

All syntheses were carried out on a vacuum line under a N_2 atmosphere. Products were isolated and handled under a N_2 atmosphere. Liquid 3-Br-pyridine, NMR solvents, and reaction solvents were stored over molecular sieves and degassed using three freeze–pump–thaw cycles under N_2 prior to use. [EtAl(2-py)$_3$]Li (**2**Li) was synthesized as described previously.[32] NMR spectra were recorded on 500 MHz Agilent DD2 and 400 MHz Agilent instruments equipped with a OneNMR probe in the Laboratory of Instrumental Techniques (LTI) Research Facilities, University of Valladolid. Chemical shifts (δ) are reported in parts per million (ppm). ^{1}H and ^{13}C NMR spectra are referenced to TMS. ^{7}Li and ^{27}Al NMR experiments are referenced to solutions of LiCl/D_2O and $AlCl_3{\cdot}6H_2O/D_2O$, respectively. All 2D ^{1}H and ^{7}Li DOSY spectra were acquired on the 500 MHz Agilent spectrometer using the 2D DOSY gradient compensated stimulated echo with convection compensation (DgcsteSL-cc) pulse sequence. Sixteen gradient levels ranging from 7 to 53 G/cm (12% to 88% of the maximum gradient strength) were used. The diffusion delay (Δ) was 50 ms and the diffusion gradient length (δ) was 2 ms (4 to 6 ms for ^{7}Li). For each DOSY NMR experiment, a series of 16 or 32 spectra was collected. Spectra were recorded in DMSO-d_6 and the temperature was set and controlled at 298 K. Coupling constants (J) are reported in Hz. Standard abbreviations are used to indicate multiplicity: s = singlet, d = doublet, t = triplet, and m = multiplet. ^{1}H and ^{13}C peak assignments were performed with the help of additional 2D NMR experiments (^{1}H–^{1}H COSY, ^{1}H–^{1}H NOESY, ^{1}H–^{13}C HSQC, ^{1}H–^{13}C HMQC, ^{1}H–^{13}C HMBC and ^{1}H–^{7}Li HOESY). High-resolution mass spectra were recorded at the mass spectrometry service of the Centro de Apoyo a la Investigación (CAI) of the University of Alcalá using an Agilent TOF-LC/MS 6210 spectrometer (ESI-TOF, negative ion mode). Elemental analysis was obtained using a CHNS-932 Elemental Analyzer at the CAI of the University of Alcalá.

Synthesis of 1Li: 3-Bromo-pyridine (0.96 mL, 10 mmol) was dissolved in diethyl ether (30 mL). To this, ^{n}BuLi (4.0 ml, 10 mmol, 2.5 M in hexane) was added dropwise over 10 min at –78 °C. The resulting yellow slurry was stirred for 15 min at –78 °C. $EtAlCl_2$ (3.7 mL, 3.33 mmol, 0.9M in hexane) was added dropwise to the light yellow lithiated species, and the resulting red mixture was allowed to reach room temperature. After overnight stirring, a solution with a red precipitate was observed. All volatiles were removed under vacuum. The resulting solid residue was dissolved in THF (20 mL) to yield a red solution, which was concentrated under vacuum, and slow diffusion of toluene (20 mL) at 8 °C over 72 h yielded [EtAl(3-py)$_3$]Li·(THF)$_2$ as colourless blocks suitable for X-ray crystallography. Isolation under vacuum (ca. 10^{-1} atm., 10 min) produced the removal of one molecule of THF and gave **1**Li·THF as an amorphous solid. The analytical results listed below correspond to this material. Yield 0.67 g (1.8 mmol, 54.2%). ^{1}H NMR (298 K, DMSO-d_6, 500 MHz): δ (ppm) = 8.54 (s, 3H, H_6 py), 8.21 (dd, J = 4.9 Hz/2.1 Hz, 3H, H_5 py), 7.74 (m, 3H, H_3 py), 7.06 (m, 3H, H_4 py), 3.60 (m, 4H, –CH_2–O, THF), 1.76 (m, 4H, –CH_2–, THF), 1.05 (t, J = 8.3 Hz, 3H, H_8), 0.1 (q, J = 8.3 Hz, 2H, H_7). ^{13}C{^{1}H} NMR (298 K, DMSO-d_6, 100.5 MHz): δ = 157.59 (C_6 py), 149.85 (br, C_2 Al–C_{py}), 146.12 (C_5 py), 145.21 (C_3 py), 122.49 (C_4 py), 66.99 (CH_2O, THF), 25.10 (–CH_2–, THF), 11.06 (C_9 py), –0.09 (br, C_7 Al-C_{Et}). ^{7}Li NMR (298 K, DMSO-d_6, 194.2 MHz, ref. solution of LiCl/D_2O): δ (ppm) = –1.09. ^{27}Al NMR (298 K, DMSO-d_6, 130.3 MHz, ref. solution of $AlCl_3{\cdot}6H_2O/D_2O$): δ (ppm) = 139.50 (br). Elemental analysis (%) calcd for [EtAl(3-py)$_3$]Li·THF ($C_{21}H_{25}AlLiN_3O$): C 68.3, H 6.8, N 11.4. Found: C 68.6, H 6.7, N 11.2. HR-MS [ESI-TOF, negative ion mode]: *m/z* for $C_{17}H_{17}AlN_3$ [**1**]$^-$ calcd: 290.1243. Found: 290.1251 (–2.65 ppm error).

Conflicts of interest

There are no conflicts to declare.

Acknowledgements

We thank the Spanish Ministry of Science, Innovation and Universities (MCIU) (project numbers PGC2018-096880-A-I00, MCIU/AEI/FEDER, UE and PGC2018-099470-B-I00, MCIU/AEI/FEDER, UE) for funding. R.G.-R. acknowledges the Spanish MINECO/AEI and the European Union (ESF) for a Ramon y Cajal contract (RYC-2015-19035) and A.G.-R. the University of Valladolid and Santander Bank for a fellowship.

References

1 L. F. Szczepura, L. M. Witham and K. J. Takeuchi, *Coord. Chem. Rev.*, 1998, **174**, 5–32.
2 A. G. Walden and A. J. M. Miller, *Chem. Sci.*, 2015, **6**, 2405–2410.
3 H. Martínez-García, D. Morales, J. Pérez, M. Puerto and I. del Río, *Chem. – Eur. J.*, 2014, **20**, 5821–5834.
4 T. Gneuß, M. J. Leitl, L. H. Finger, N. Rau, H. Yersin and J. Sundermeyer, *Dalton Trans.*, 2015, **44**, 8506–8520.
5 A. Maleckis, J. W. Kampf and M. S. Sanford, *J. Am. Chem. Soc.*, 2013, **135**, 6618–6625.
6 N. M. Camasso and M. S. Sanford, *Science*, 2015, **347**, 1218–1220.
7 J. Gülzow, G. Hörner, P. Strauch, A. Stritt, E. Irran and A. Grohmann, *Chem. – Eur. J.*, 2017, **23**, 7009–7023.

8 J. S. Derrick, M. Loipersberger, R. Chatterjee, D. A. Iovan, P. T. Smith, K. Chakarawet, J. Yano, J. R. Long, M. Head-Gordon and C. J. Chang, *J. Am. Chem. Soc.*, 2020, **142**, 20489–20501.

9 M. Kodera, K. Katayama, Y. Tachi, K. Kano, S. Hirota, S. Fujinami and M. Suzuki, *J. Am. Chem. Soc.*, 1999, **121**, 11006–11007.

10 C. Y. Liu, X. R. Chen, H. X. Chen, Z. Niu, H. Hirao, P. Braunstein and J. P. Lang, *J. Am. Chem. Soc.*, 2020, **142**, 6690–6697.

11 M. K. Wojnar, D. W. Laorenza, R. D. Schaller and D. E. Freedman, *J. Am. Chem. Soc.*, 2020, **142**, 14826–14830.

12 S. Treiling, C. Wang, C. Förster, F. Reichenauer, J. Kalmbach, P. Boden, J. P. Harris, L. M. Carrella, E. Rentschler, U. Resch-Genger, C. Reber, M. Seitz, M. Gerhards and K. Heinze, *Angew. Chem., Int. Ed.*, 2019, **58**, 18075–18085.

13 H. R. Simmonds and D. S. Wright, *Chem. Commun.*, 2012, **48**, 8617–8624.

14 A. J. Plajer, A. L. Colebatch, M. Enders, Á. García-Romero, A. D. Bond, R. García-Rodríguez and D. S. Wright, *Dalton Trans.*, 2018, **47**, 7036–7043.

15 F. Reichart, M. Kischel and K. Zeckert, *Chem. – Eur. J.*, 2009, **15**, 10018–10020.

16 K. Zeckert, S. Zahn and B. Kirchner, *Chem. Commun.*, 2010, **46**, 2638–2640.

17 K. Zeckert, J. Griebel, R. Kirmse, M. Weiß and R. Denecke, *Chem. – Eur. J.*, 2013, **19**, 7718–7722.

18 I. Schrader, K. Zeckert and S. Zahn, *Angew. Chem., Int. Ed.*, 2014, **53**, 13698–13700.

19 A. J. Peel, J. E. Waters, A. J. Plajer, R. García-Rodríguez and D. S. Wright, *Adv. Organomet. Chem.*, 2021, **75**, 193–244.

20 A. J. Plajer, A. L. Colebatch, F. J. Rizzuto, P. Pröhm, A. D. Bond, R. García-Rodríguez and D. S. Wright, *Angew. Chem., Int. Ed.*, 2018, **57**, 6648–6652.

21 Á. García-Romero, A. J. Plajer, D. Miguel, D. S. Wright, A. D. Bond, C. M. Álvarez and R. García-Rodríguez, *Inorg. Chem.*, 2020, **59**, 7103–7116.

22 A. J. Plajer, D. Crusius, R. B. Jethwa, Á. García-Romero, A. D. Bond, R. García-Rodríguez and D. S. Wright, *Dalton Trans.*, 2021, **50**, 2393–2402.

23 J. C. Thomas and J. C. Peters, *J. Am. Chem. Soc.*, 2003, **125**, 8870–8888.

24 A. Steiner and D. Stalke, *J. Chem. Soc. Chem. Commun.*, 1993, 1702–1704.

25 B. D. Matson and J. C. Peters, *ACS Catal.*, 2018, **8**, 1448–1455.

26 T. J. Del Castillo, N. B. Thompson and J. C. Peters, *J. Am. Chem. Soc.*, 2016, **138**, 5341–5350.

27 F. García, A. D. Hopkins, R. A. Kowenicki, M. McPartlin, M. C. Rogers and D. S. Wright, *Organometallics*, 2004, **23**, 3884–3890.

28 S. Y. Jeong, R. A. Lalancette, H. Lin, P. Lupinska, P. O. Shipman, A. John, J. B. Sheridan and F. Jäkle, *Inorg. Chem.*, 2016, **55**, 3605–3615.

29 K. Zeckert and D. Fuhrmann, *Inorg. Chem.*, 2019, **58**, 16736–16742.

30 C. Cui, R. A. Lalancette and F. Jäkle, *Chem. Commun.*, 2012, **48**, 6930–6932.

31 T. H. Bullock, W. T. K. Chan and D. S. Wright, *Dalt. Trans.*, 2009, 6709–6711.

32 T. H. Bullock, W. T. K. Chan, D. J. Eisler, M. Streib and D. S. Wright, *Dalton Trans.*, 2009, **6**, 1046–1054.

33 C. S. Alvarez, F. García, S. M. Humphrey, A. D. Hopkins, R. A. Kowenicki, M. McPartlin, R. A. Layfield, R. Raja, M. C. Rogers, A. D. Woods and D. S. Wright, *Chem. Commun.*, 2005, 198–200.

34 F. García, A. D. Hopkins, R. A. Kowenicki, M. McPartlin, M. C. Rogers, J. S. Silvia and D. S. Wright, *Organometallics*, 2006, **25**, 2561–2568.

35 R. García-Rodríguez, T. H. Bullock, M. McPartlin and D. S. Wright, *Dalton Trans.*, 2014, **43**, 14045–14053.

36 R. García-Rodríguez, H. R. Simmonds and D. S. Wright, *Organometallics*, 2014, **33**, 7113–7117.

37 R. García-Rodríguez, S. Kopf and D. S. Wright, *Dalton Trans.*, 2018, **47**, 2232–2239.

38 R. García-Rodríguez and D. S. Wright, *Chem. – Eur. J.*, 2015, **21**, 14949–14957.

39 R. García-Rodríguez, S. Hanf, A. D. Bond and D. S. Wright, *Chem. Commun.*, 2017, **53**, 1225–1228.

40 Á. García-Romero, A. J. Plajer, L. Álvarez-Miguel, A. D. Bond, D. S. Wright and R. García-Rodríguez, *Chem. – Eur. J.*, 2018, **24**, 17019–17026.

41 A. J. Plajer, S. Kopf, A. L. Colebatch, A. D. Bond, D. S. Wright and R. García-Rodríguez, *Dalton Trans.*, 2019, **48**, 5692–5697.

42 R. García-Rodríguez and D. S. Wright, *Dalton Trans.*, 2014, **43**, 14529–14532.

43 A. M. Kluwer, R. Kapre, F. Hartl, M. Lutz, A. L. Spek, A. M. Brouwer, P. W. N. M. Van Leeuwen and J. N. H. Reek, *Proc. Natl. Acad. Sci. U. S. A.*, 2009, **106**, 10460–10465.

44 L. Dubován, A. Pöllnitz and C. Silvestru, *Eur. J. Inorg. Chem.*, 2016, **10,** 1521–1527.

45 R. Zaffaroni, W. I. Dzik, R. J. Detz, J. I. van der Vlugt and J. N. H. Reek, *Eur. J. Inorg. Chem.*, 2019, **2019**, 2498–2509.

46 V. Bocokić, A. Kalkan, M. Lutz, A. L. Spek, D. T. Gryko and J. N. H. Reek, *Nat. Commun.*, 2013, **4**, 2670.

47 M. S. Deshmukh, A. Yadav, R. Pant and R. Boomishankar, *Inorg. Chem.*, 2015, **54**, 1337–1345.

48 E. S. Yang, A. J. Plajer, A. Garcia-Romero, A. D. Bond, T. K. Ronson, C. M. Alvarez, R. Garcia-Rodriguez, A. L. Colebatch and D. S. Wright, *Chem. – Eur. J.*, 2019, **25**, 14003-14009

49 L. J. Jongkind, J. A. A. W. Elemans and J. N. H. Reek, *Angew. Chem. Int. Ed.,* 2019, **58**, 2696–2699.

50 K. S. Kumar, V. S. Mane, A. Yadav, A. S. Kumbhar and

R. Boomishankar, *Chem. Commun.*, 2019, **55**, 13156–13159.
51 M. S. Deshmukh, V. S. Mane, A. S. Kumbhar and R. Boomishankar, *Inorg. Chem.*, 2017, **56**, 13286–13292.
52 I. Jacobs, A. C. T. Van Duin, A. W. Kleij, M. Kuil, D. M. Tooke, A. L. Spek and J. N. H. Reek, *Catal. Sci. Technol.*, 2013, **3**, 1955–1963.
53 V. F. Slagt, P. C. J. Kamer, P. W. N. M. Van Leeuwen and J. N. H. Reek, *J. Am. Chem. Soc.*, 2004, **126**, 1526–1536.
54 D. Li, I. Keresztes, R. Hopson and P. G. Williard, *Acc. Chem. Res.*, 2009, **42**, 270–280.
55 D. Li, G. Kagan, R. Hopson and P. G. Williard, *J. Am. Chem. Soc.*, 2009, **131**, 5627–5634.
56 R. Neufeld and D. Stalke, *Chem. Sci.*, 2015, **6**, 3354–3364.
57 S. Bachmann, R. Neufeld, M. Dzemski and D. Stalke, *Chem. – Eur. J.*, 2016, **22**, 8462–8465.
58 S. Bachmann, B. Gernert and D. Stalke, *Chem. Commun.*, 2016, **52**, 12861–12864.
59 R. Tatara, D. G. Kwabi, T. P. Batcho, M. Tulodziecki, K. Watanabe, H. M. Kwon, M. L. Thomas, K. Ueno, C. V. Thompson, K. Dokko, Y. Shao-Horn and M. Watanabe, *J. Phys. Chem. C*, 2017, **121**, 9162–9172.
60 S. D. Robertson, M. Uzelac and R. E. Mulvey, *Chem. Rev.*, 2019, **119**, 8332–8405.
61 R. E. Mulvey and S. D. Robertson, *Top. Organomet. Chem.*, 2013, **47**, 129–158.

Synthesis of tris(3-pyridyl)aluminate ligand and its unexpected stability against hydrolysis: revealing cooperativity effects in heterobimetallic pyridyl aluminates

A. Garcia-Romero J. M. Martín-Álvarez, A. L. Colebatch, A. J. Plajer, D. Miguel, C. M. Álvarez and R. García-Rodríguez ·

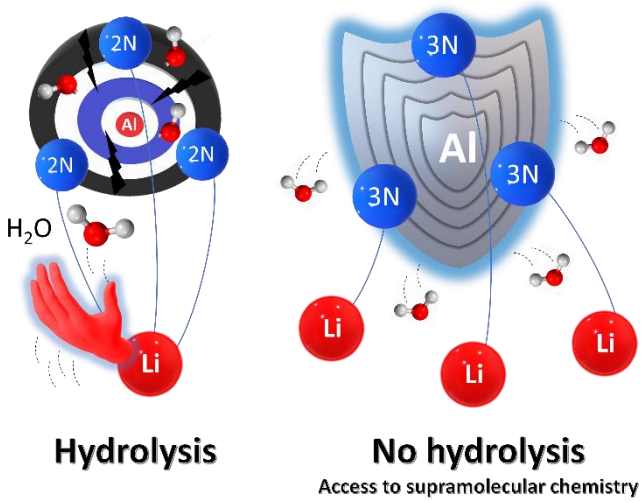

Bimetallic cooperativity provides a reason for the unexpected water stability of the tris(3-pyridyl)aluminate $[EtAl(3\text{-py})_3]^-$ (3-py = 3-pyridyl) (**1**), the first reported member of the anionic tris(3-pyridyl) ligand family.